wild-type plants in blue light can be at least partially explained by the absence of the activity of the red-light–dependent inhibitors, phytochromes. Under white light or blue-plus-red light, red-light–dependent phytochrome activity and blue-light–dependent cry2 activity function in an antagonistic manner. In these light conditions, *cry2* mutant plants flower late because the red-light–dependent phytochrome activity inhibiting floral initiation remains untamed as a result of the lack of the blue-light–dependent cry2 activity in the mutant plants.

We suggest that the function of both phytochromes and cry2 in flowering-time regulation are mediated by CO. The function of phytochromes proposed in our model is consistent with the observation that *Arabidopsis hy1* and *hy2* mutants, defective in the biosynthesis of phytochrome chromophore, flower earlier than the wild-type plants (6). It is not clear how many phytochrome species are involved in mediating red-light–dependent inhibition of flowering, although phyA is probably not associated with the flowering inhibition because the phyA mutant does not flower early (6). *phyB* mutant plants flower earlier than the wild-type plants grown under white light (6, 7), an effect mediated by CO (20). Thus, phyB could be one of the phytochromes that mediates red-light–dependent inhibition of flowering (4). Indeed, the early-flowering phenotype of *phyB* is dependent on red light (Fig. 4). In blue light, however, *phyB* mutant plants flowered at about the same time as the wild type (Fig. 4; blue). Consistent with our model, *phyB* mutation can suppress the late-flowering phenotype of *cry2* under blue-plus-red light, whereas the *cry2* mutation cannot suppress the early-flowering phenotype of *phyB* in red light (26).

Although our model explains the mode of action of cry2 and phyB in the regulation of flowering time of *Arabidopsis*, phyA and cry1 appear to function in different ways in this process (6, 8, 9), and the relative importance of individual photoreceptors in mediating photoperiodic signals may be different in other plant species (9). It will also be interesting to learn the relationship between cry2 in photoperiodism and the circadian clock associated with blue-light–entrained circadian rhythms in plants (27).

REFERENCES AND NOTES

1. R. E. Kendrick and G. H. M. Kronenberg, *Photomorphogenesis in Plants* (Kluwer Academic, Dordrecht, ed. 2, 1994); H. Mohr, *ibid.*, pp. 353–373; H. Smith, *Annu. Rev. Plant Physiol. Plant Mol. Biol.* **46**, 289 (1995); M. Furuya and E. Schafer, *Trends Plant Sci.* **1**, 301 (1996); A. von Arnim and X.-W. Deng, *Annu. Rev. Plant Physiol. Plant Mol. Biol.* **47**, 215 (1996).
2. W. Briggs, R. L. Health, E. Tobin, *Regulation of Plant Growth and Development by Light*, vol. 17 of *Current Topics in Plant Physiology* (American Society of Plant Physiologists, Rockville, MD, 1996).
3. P. H. Quail *et al.*, *Science* **268**, 675 (1995).
4. J. Chory, *Plant Cell* **9**, 1225 (1997).
5. M. Ahmad and A. R. Cashmore, *Nature* **366**, 162 (1993); E. Liscum and R. P. Hangarter, *Plant Cell Env.* **17**, 639 (1994); C. Lin *et al.*, *Science* **269**, 968 (1995); M. Ahmad and A. R. Cashmore, *Plant Mol. Biol.* **30**, 851 (1996); C. Lin and A. R. Cashmore, in (2), pp. 30–39.
6. N. Goto, T. Kumagai, M. Koornneef, *Physiol. Plant.* **83**, 209 (1991).
7. J. W. Reed, P. Nagpal, D. S. Poole, M. Furuya, J. Chory, *Plant Cell* **5**, 147 (1993).
8. D. J. Bagnall *et al.*, *Plant Physiol.* **108**, 1495 (1995); D. J. Bagnall, R. W. King, R. P. Hangarter, *Planta* **200**, 278 (1996); R. King and D. Bagnall, *Semin. Cell Dev. Biol.* **7**, 449 (1996); M. T. Zagotta *et al.*, *Plant J.* **10**, 691 (1996).
9. E. Johnson, M. Bradley, N. P. Harberd, G. C. Whitelam, *Plant Physiol.* **105**, 141 (1994); K. J. Halliday, M. Koornneef, G. C. Whitelam, *ibid.* **104**, 1311 (1994); J. L. Weller, I. C. Murfet, J. B. Reid, *ibid.* **114**, 1225 (1997); J. L. Weller, J. B. Reid, S. A. Taylor, I. C. Murfet, *Trends Plant Sci.* **2**, 412 (1997).
10. C. Lin *et al.*, *Proc. Natl. Acad. Sci. U.S.A.* **95**, 2686 (1998).
11. The strategy used in the isolation of the *cry2* mutant is based on the observation that overexpression of CRY2 resulted in a short hypocotyl under blue light, especially low intensity of blue light (*10*). Fast-neutron–mutagenized Columbia (Col-4) seeds were sown on compound soil, kept in a cold room (4°C) in the dark for 4 days, exposed to ~150 μmol s^{-1} m^{-2} of cool white fluorescent light for 1 day, and grown under low intensity of blue light (2 to 5 μmol s^{-1} m^{-2}) for 2 to 3 days. Seedlings that grew taller than average were selected. Individual isolates were analyzed for the CRY2 expression using the immunoblot assay (*10*). Two *cry2* alleles were identified from 636 isolates initially selected from ~130,000 M_2 seeds. Lights and filters used are as described (*10*).
12. M. Koornneef, C. J. Hanhart, J. H. van der Veen, *Mol. Gen. Genet.* **229**, 57 (1991).
13. J. M. Martinez-Zapater, G. Coupland, C. Dean, M. Koornneef, in Arabidopsis, E. M. Meyerowitz and C. R. Somerville, Eds. (Cold Spring Harbor Laboratory Press, Cold Spring Harbor, NY, 1994), pp. 403–433; R. Simon and G. Coupland, *Semin. Cell Dev. Biol.* **7**, 419 (1996); A. J. M. Peeters and M. Koornneef, *ibid.*, p. 381; K. A. Hicks, A. Sundas, D. R. Meeks-Wagner, *ibid.*, p. 409; M. Aukerman and R. M. Amasino, *ibid.*, p. 427; H. Ma, *Cell* **89**, 821 (1997); M. Koornneef, C. Alonso-Blanco, A. J. M. Peeters, W. Soppe, *Annu. Rev. Plant Physiol. Plant Mol. Biol.*, in press).
14. G. Coupland, *Trends Genet.* **11**, 393 (1995).
15. D. Bradley, O. Ratcliffe, C. Vincent, R. Carpenter, E. Coen, *Science* **275**, 80 (1997).
16. G. Redei, *Genetics* **47**, 443 (1962).
17. The BAC clone F19P19 containing the *CRY2* gene (http://pgec-genome.pw.usda. gov/libraries.html) is located at the 0846 locus, about 5 centimorgans from the *PHYA* gene in the recombinant inbred map (http://cbil.humgen.upenn.edu/~atgc/ATGCUP.html or http://nasc.nott.ac.uk/new_ri_map.html). FHA was mapped to about 4 centimorgans from the *PHYA* gene in the classical genetic map (http://mutant.lse.okstate.edu/genepage/classical_map.html) (*12*). For the complementation test, the flowering time of F_1 progenies of *cry2-1* (Col background) × *fha-1* (Ler background) was compared with that of the F_1 progenies of *cry2-1* × Ler and Col × *fha-1*.
18. D. S. Hsu *et al.*, *Biochemistry* **35**, 13871 (1996).
19. H.-W. Park, S.-T. Kim, A. Sancar, J. Deisenhofer, *Science* **268**, 1866 (1995).
20. J. Putterill, F. Robson, K. Lee, R. Simon, G. Coupland, *Cell* **80**, 847 (1995).
21. T. Araki and Y. Komeda, *Plant J.* **3**, 231 (1993).
22. R. Simon, M. I. Igeno, G. Coupland, *Nature* **384**, 59 (1996).
23. K. D. Jofuku *et al.*, *Plant Cell* **6**, 1211 (1994).
24. J. A. M. Brown and W. H. Klein, *Plant Physiol.* **47**, 393 (1971).
25. K. Eskins, *Physiol. Plant.* **86**, 439 (1992).
26. T. Mockler and C. Lin, unpublished data.
27. A. J. Millar, M. Straume, J. Chory, N.-H. Chua, S. A. Kay, *Science* **267**, 1163 (1995).
28. M. Aitchitt *et al.*, *Plant Mol. Biol. Rep.* **11**, 317 (1993).
29. Single-letter abbreviations for the amino acid residues are as follows: E, Glu; F, Phe; G, Gly; H, His; I, Ile; K, Lys; M, Met; R, Arg; S, Ser; and W, Trp.

30. We thank W. Yang, H. Duong, N. Ma, and J. Chen, for their assistance in the experiments, S. Poethig and S. Nourizadeh for providing the fast-neutron–mutagenized seeds, G. Coupland for providing DNA probes for the analysis of *CO* expression, M. Neff and J. Chory for providing the *phyB* mutant seeds, and E. Tobin for the critical readings of the manuscript. C.L. would like to thank A. Cashmore for continuous encouragement and support which made this work possible. Supported in part by UCLA (start-up fund to C.L.) and NIH (GM56265 to C.L.). T.M. is partially supported by a predoctoral fellowship (GM08375) from NIH.

22 October 1997; accepted 6 January 1998

Src Activation in the Induction of Long-Term Potentiation in CA1 Hippocampal Neurons

You Ming Lu, John C. Roder,* Jonathan Davidow, Michael W. Salter

Long-term potentiation (LTP) is an activity-dependent strengthening of synaptic efficacy that is considered to be a model of learning and memory. Protein tyrosine phosphorylation is necessary to induce LTP. Here, induction of LTP in CA1 pyramidal cells of rats was prevented by blocking the tyrosine kinase Src, and Src activity was increased by stimulation producing LTP. Directly activating Src in the postsynaptic neuron enhanced excitatory synaptic responses, occluding LTP. Src-induced enhancement of α-amino-3-hydroxy-5-methylisoxazolepropionic acid (AMPA) receptor–mediated synaptic responses required raised intracellular Ca^{2+} and *N*-methyl-D-aspartate (NMDA) receptors. Thus, Src activation is necessary and sufficient for inducing LTP and may function by up-regulating NMDA receptors.

Long-term potentiation is a persistent enhancement in the efficacy of synaptic transmission that has been proposed to be a principal cellular substrate underlying learning and memory (1). LTP is induced by a cascade of biochemical steps that, for a main form of LTP, occur in the postsynaptic neuron (2). Protein tyrosine phosphorylation is

necessary for induction of LTP (3); however, it has not been determined which of the many tyrosine kinases expressed in the central nervous system (CNS) is essential for LTP induction (4), and the role of the kinase is unclear. Tyrosine phosphorylation regulates the function of NMDA receptors (5), which are necessary for induction of LTP at many synapses (6). The regulation of NMDA receptors by tyrosine phosphorylation is via the nonreceptor protein tyrosine kinase Src (7). Thus, we set out to determine whether Src participates in LTP.

We made whole-cell patch-clamp recordings from pyramidal neurons in the CA1 region of hippocampal slices from rat brains; field potentials were recorded by an extracellular electrode (8). Excitatory synaptic responses were evoked by stimulating the Schaffer collateral inputs to CA1 neurons. LTP at these synapses is known to depend on NMDA receptors (6). In order to determine whether Src is necessary for LTP induction, we made use of a unique domain peptide fragment, Src(40–58), which is known to block Src function (7). Src(40–58) was applied directly into the neurons by diffusional exchange from the patch electrode (Fig. 1A). During application of Src(40–58), tetanic stimulation caused short-term but not long-lasting potentiation of the intracellularly recorded excitatory postsynaptic potentials (EPSPs): the slope of the EPSPs was 99 ± 5.7% (mean ± SEM) of the baseline level by 30 min after tetanic stimulation (n = 6 cells). However, the tetanic stimulation did produce a long-lasting increase in field EPSP slope to 182 ± 24% of baseline. Thus, Src(40–58) prevented induction of LTP in the cells in which it was administered intracellularly, but not in neighboring cells. A peptide with the same amino acid composition, but in random order, scrambled Src(40–58), served as a control (9), and did not prevent induction of LTP. Intracellular application of the antibody anti-Src1, which specifically blocks Src action (10), caused the EPSP slope to decline to 120 ± 9.5% of baseline by 30 min after tetanus (n = 7 cells; Fig. 1B), whereas the field EPSP slope was at a sustained level of 189 ± 21% of baseline. In contrast, a nonspecific immunoglobulin G (IgG) fraction did not affect LTP induction. With administration of Src(40–58) or of anti-Src1, the tetanic stimulation produced posttetanic potentiation, the peak of which was not different from that of the respective controls. Thus, Src was necessary for induction of LTP.

In the adult CNS, there is a basal level of Src activity (4), and in CA1 neurons this might produce a tonic enhancement of NMDA channel function. Then the blockade of LTP might have been through abolishing ongoing enhancement of NMDA channels, in which case blocking Src would be expected to reduce basal synaptic NMDA responses. However, in voltage-clamp experiments (11), administration of Src(40–58) had no effect on pharmacologically isolated NMDA receptor–mediated excitatory postsynaptic currents (NMDAR EPSCs) (Fig. 1C). Moreover, Src(40–58) had no effect on AMPA receptor–mediated

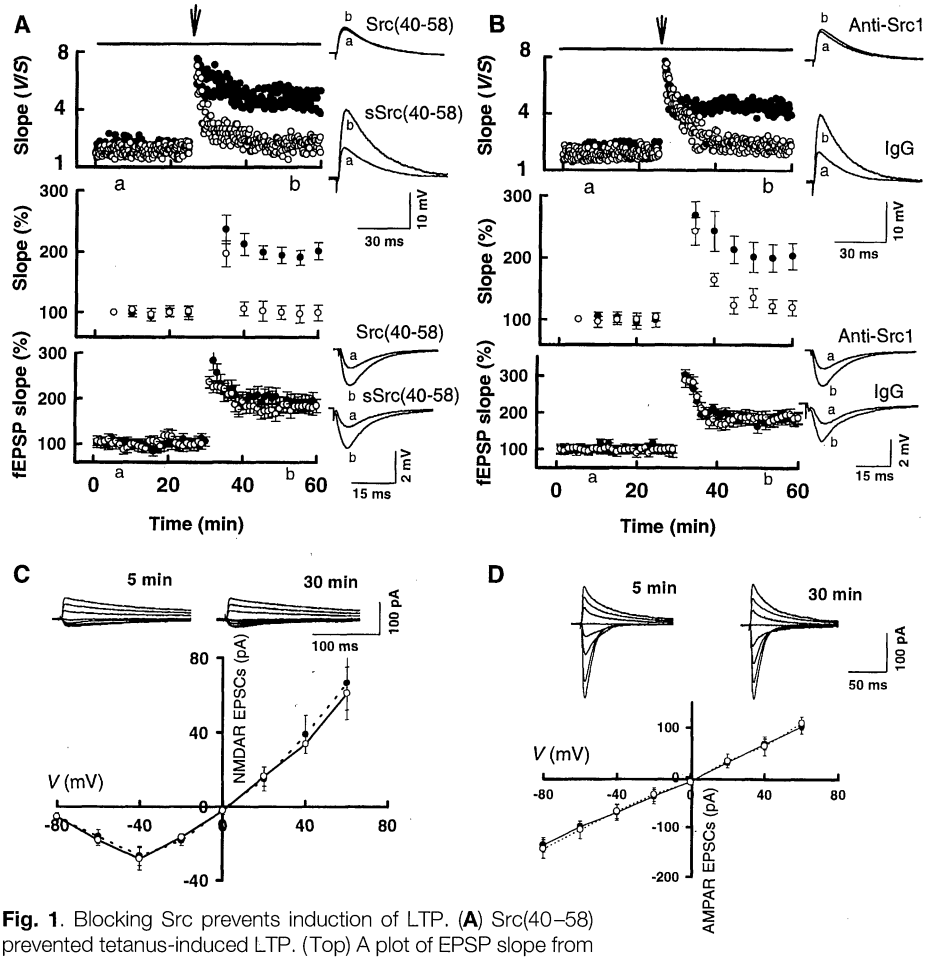

Fig. 1. Blocking Src prevents induction of LTP. (**A**) Src(40–58) prevented tetanus-induced LTP. (Top) A plot of EPSP slope from representative cells with intracellular administration of Src(40–58) (○) or scrambled Src(40–58) [sSrc(40–58), ●]. (Middle) Averaged EPSP slope for experiments with Src(40–58) (○, n = 6) or sSrc(40–58) (●, n = 5). Data were normalized to baseline values (8). (Bottom) Averaged normalized field EPSP (fEPSP) slope with Src(40–58) (○) or sSrc(40–58) (●). (**B**) Anti-Src1 inhibited tetanus-induced LTP. (Top) EPSP slope plotted for example cells in which anti-Src1 (○) or a nonspecific IgG fraction (●) was administered. (Middle) Averaged normalized EPSP slope for recordings with application of anti-Src1 (○, n = 7) or a nonspecific IgG fraction (●, n = 4). (Bottom) Averaged normalized fEPSP slope with anti-Src1 (○) or nonspecific IgG (●). (**C**) Src(40–58) had no effect on basal NMDAR EPSCs. (Top) Traces from a cell with intracellular administration of Src(40–58) and bath application of CNQX. Each trace is the average of three EPSCs evoked at membrane potentials from −80 to +60 mV, in 20-mV increments. The I-V relation was determined during the first 5-min period (left) or 30 min after the start of recording (right). (Bottom) I-V relation for averaged amplitudes of NMDAR EPSCs (n = 3) during the first 5 min (○) and the period from 30 to 35 min (●). (**D**) Src(40–58) had no effect on basal AMPAR EPSCs. (Top) EPSCs from a cell recorded with administration of Src(40–58) but without CNQX. Each trace is the average of two responses evoked at membrane potentials from −80 to +60 mV, from the first 5 min (left) or at 30 min (right) after the start of recording. (Bottom) Averaged I-V relation for peak amplitude of AMPAR EPSCs (n = 3) from the first 5 min (○) or for 30 to 35 min (●). In Figs. 1 through 4, horizontal bars above the graphs indicate the periods of peptide administration and the arrow indicates the time of tetanic stimulation. Error bars are ±SEM, and the traces to the right of the graphs are averages of three sweeps taken at the time points indicated by the letters below the x axis.

Y. M. Lu and J. C. Roder, Samuel Lunenfeld Research Institute, Mount Sinai Hospital, and Department of Molecular and Medical Genetics, University of Toronto, M5S 1A8, Canada.
J. Davidow and M. W. Salter, Division of Neuroscience, Hospital for Sick Children, and Department of Physiology, University of Toronto, M5G 1X8, Canada. E-mail: mike.salter@utoronto.ca

*To whom correspondence should be addressed. E-mail: roder@mshri.on.ca

(AMPAR) EPSCs (Fig. 1D). Thus, neither synaptic NMDARs nor synaptic AMPARs were enhanced tonically by basal Src function.

We hypothesized that Src might be activated during LTP induction. To test this, we measured Src catalytic activity by means of an immune-complex kinase assay (*12*).

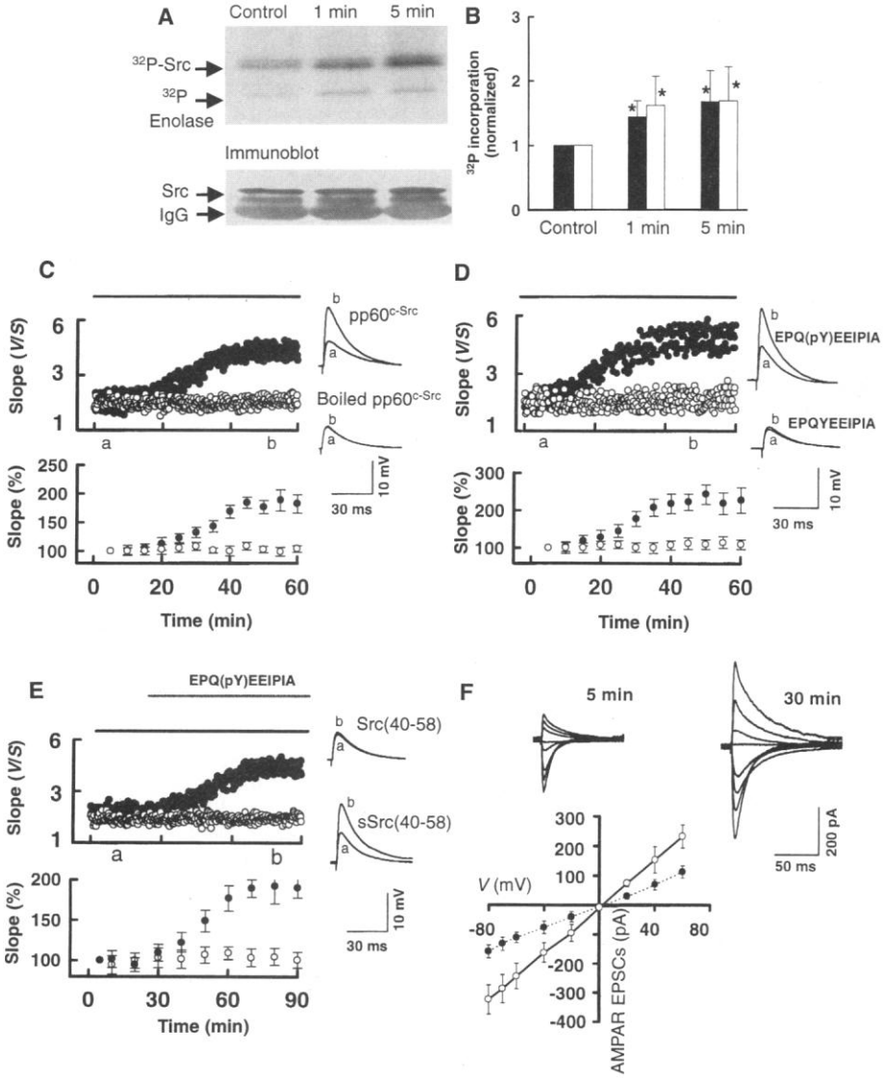

Fig. 2. Src activity is increased by tetanic stimulation, and activation of endogenous Src causes synaptic potentiation. (**A**) Immune complex kinase assays were done with Src immunoprecipitated after control stimulation or 1 min or 5 min after tetanus. Proteins were separated by SDS-PAGE and transferred to nitrocellulose, and ^{32}P was detected by exposure to a Phosphor Screen. Results of a representative immune complex kinase experiment are shown; phosphorylation of Src or of enolase is indicated by the arrows. The corresponding anti-Src immunoblot is shown below. (**B**) ^{32}P labeling was quantified for Src (solid bars) and enolase (open bars). Data from 1- and 5-min times were normalized as a percentage of control (n = 4 experiments). (**C**) (Top) A plot of EPSP slope during intracellular application of pp60$^{c\text{-}Src}$ (●) or heat-inactivated (boiled) pp60$^{c\text{-}Src}$ (○). (Bottom) Averaged EPSP slope with application of pp60$^{c\text{-}Src}$ (n = 7) or boiled pp60$^{c\text{-}Src}$ (n = 5). (**D**) (Top) A plot of EPSP slope during intracellular application of EPQ(pY)EEIPIA (1 mM, ●), or EPQYEEIPIA (1 mM, ○). Neither EPQ(pY)EEIPIA nor EPQYEEIPIA affected resting membrane potential or input resistance (not shown in figure). (Bottom) Averaged EPSP slope during application of EPQ(pY)EEIPIA (n = 8) or EPQYEEIPIA (n = 4). (**E**) (Top) A record of EPSP slope during intracellular application of Src(40–58) (○) or sSrc(40–58) (●). During the period indicated by the upper horizontal line, EPQ(pY)EEIPIA was administered by perfusion of the patch electrode. (Bottom) Averaged effects of EPQ(pY)EEIPIA on EPSP slope during application of Src(40–58) (○, n = 6) or sSrc(40–58) (●, n = 5). (**F**) *I-V* relations for EPSCs evoked during application of EPQ(pY)EEIPIA. EPSCs were evoked at membrane potentials from −80 to +60 mV. (Top) The records are superimposed EPSC traces collected during the first 5 or 30 min after the start of recording. (Bottom) Averaged peak amplitudes of AMPAR EPSCs are plotted in the graph (n = 4 cells) for the first 5 min (●) or at 30 min (○).

The ^{32}P incorporation produced by Src immunopurified from slices that had received tetanic stimulation was greater than that from control slices that had received only test stimulation (Fig. 2, A and B). Because there was no difference in the level of Src protein (Fig. 2A), tetanus caused an increase in Src activity.

To determine whether increasing Src activity affects synaptic responses, we administered exogenous recombinant Src (pp60$^{c\text{-}Src}$), which was found to increase EPSP slope to 185 ± 24% of baseline (n = 7 cells). In contrast, heat-inactivated pp60$^{c\text{-}Src}$ had no effect (Fig. 2C). To examine the effect of activating endogenous Src, we used the high-affinity peptide EPQ(pY)EEIPIA (*13*), which is an activator of tyrosine kinases in the Src family (*14*). EPQ(pY)EEIPIA was applied alone or with Src(40–58) to determine whether the effects required Src itself. Application of EPQ(pY)EEIPIA produced an increase in EPSP slope to a sustained level at 226 ± 22% of baseline (n = 8 cells; Fig. 2D). On the other hand, the nonphosphorylated form of the peptide, EPQYEEIPIA, which does not activate tyrosine kinases (*14*), did not affect EPSPs (n = 4 cells). Moreover, during administration of Src(40–58), perfusion with EPQ(pY)EEIPIA (*15*) had no effect on EPSP slope (n = 6 cells, Fig. 2E). But during administration of scrambled Src(40–58), perfusion of EPQ(pY)EEIPIA did produce an increase in EPSP slope to 200 ± 19% of baseline (n = 5 cells). Thus, endogenous Src was necessary for the enhancement of EPSPs by EPQ(pY)EEIPIA. In voltage-clamp recordings, EPQ(pY)EEIPIA potentiated AMPAR EPSCs through an increase in AMPAR EPSC conductance, with no change in driving force (Fig. 2F). Overall, activation of Src was sufficient to enhance EPSPs.

If endogenous Src participates in LTP produced by tetanic stimulation, then LTP and the enhancement by the activating peptide may occlude each other. This was investigated by applying EPQ(pY)EEIPIA, and when the EPSPs had been maximally enhanced tetanic stimulation was delivered (Fig. 3A). This stimulation caused posttetanic potentiation but produced no long-lasting increase in EPSP slope. In contrast, when EPQYEEIPIA was administered, delivering tetanic stimulation at the same time after beginning the recording caused a long-lasting increase in EPSP slope (212 ± 5.3% of baseline, n = 5 cells). In other experiments, tetanus produced a lasting potentiation of EPSP slope (212 ± 28% of baseline, n = 5 cells), but there was no further increase when EPQ(pY)EEIPIA was applied intracellularly (Fig. 3B). On the other hand, in cells not

conditioned by tetanic stimulation, perfusion of EPQ(pY)EEIPIA at the same time after beginning recording caused a progressive enhancement of EPSP slope that reached a stable level at 225 ± 23% of baseline (n = 4 cells). Thus, Src-induced enhancement of EPSPs and tetanus-induced LTP were mutually occluded.

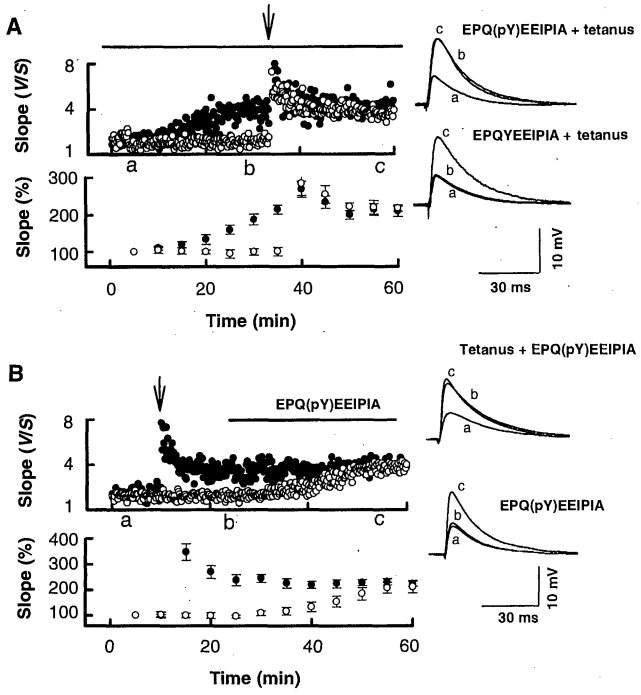

Fig. 3. Src-induced potentiation and LTP occlude each other. (**A**) Effect of tetanic stimulation (arrow) during intracellular application of EPQ(pY)EEIPIA (1 mM, ●) or EPQYEEIPIA (1 mM, ○). Recordings of EPSP slope during application of EPQ(pY)-EEIPIA (n = 5) or EPQYEEIPIA (n = 5) from representative cells are plotted at the top. The averaged EPSP slope is shown in the graph in the bottom. (**B**) Effect of tetanus (arrow) on action of EPQ(pY) EEIPIA. Representative recordings of EPSP slope when tetanus was delivered 10 min after the start of recording (●) or without tetanus (○) are shown in the top graph. EPQ(pY)EEIPIA (1 mM) was actively perfused during the period indicated by the horizontal bar above the top graph. The averaged EPSP slope is plotted in the bottom graph (n = 5 with tetanus, n = 4 without tetanus). Neither EPQ(pY)EEIPIA nor EPQYEEIPIA affected the tetanus-induced potentiation of the fEPSP slope.

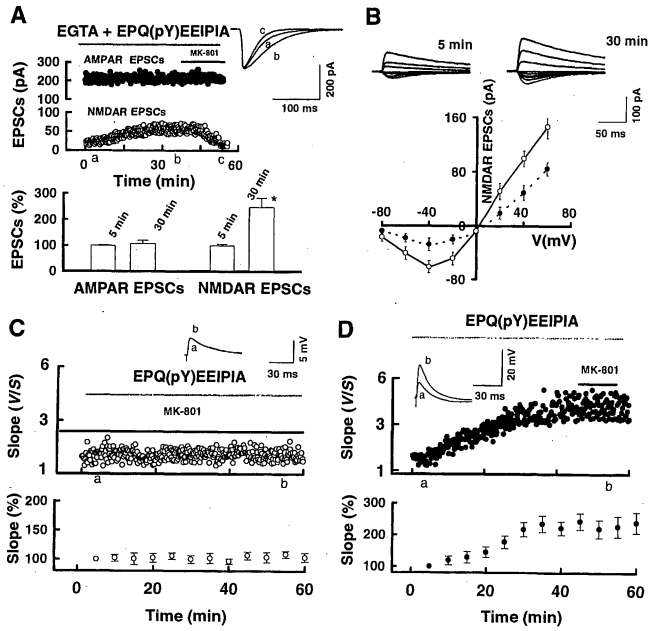

Fig. 4. Src-induced enhancement of synaptic AMPAR responses depends on raising intracellular [Ca^{2+}] and on NMDARs. (**A**) Potentiation of AMPAR EPSCs is Ca^{2+}-dependent, but potentiation of the NMDAR EPSC component is Ca^{2+}-independent. (Top) Plot of amplitude of AMPAR EPSCs (●) and the NMDAR component (○) during a recording with high Ca^{2+}-buffering intracellular solution and application of EPQ(pY)EEIPIA. The short bar indicates the period of bath application of MK-801 (10 μM). The NMDAR component was measured 100 ms after the stimulation. (Bottom) Effect of EPQ(pY)-EEIPIA on averaged AMPAR ESPCs or the NMDAR component during recordings with high Ca^{2+}-buffering intracellular solution (n = 5). Data were normalized to EPSCs in the first minute of recording. (**B**) I-V relation for pharmacologically isolated NMDAR EPSCs during application of EPQ(pY)EEIPIA. (Top) Superimposed NMDAR EPSCs evoked at membrane potentials from −80 to +60 mV. Traces are from the first 5 min and after 30 min of recording. (Bottom) Averaged amplitudes of NMDAR EPSCs (n = 3 cells) from the first 5 min (●) or after 30 min (○). (**C**) MK-801 (10 μM) was bath-applied just before the start of recording with intracellular solution containing EPQ(pY)EEIPIA. The upper graph shows a representative plot of EPSP slope from one cell, and the lower graph is averaged normalized data (n = 4). (**D**) EPQ(pY)EEIPIA was administered intracellularly and MK-801 (10 μM) was bath-applied during the period indicated by the short horizontal line, after the potentiation of EPSP slope was established. One example is shown in the upper graph and the averaged normalized EPSP slope is plotted below (n = 5).

Because LTP in CA1 neurons depends on raising the intracellular concentration of Ca^{2+} (*16*), we next determined whether the Src-induced enhancement of AMPAR EPSCs might be linked to a rise in [Ca^{2+}]. In previous experiments, AMPA receptors appeared not to be regulated by Src (*7*), but in those experiments, in contrast to the present ones, a high level of intracellular Ca^{2+} buffering was used. To determine whether Src-induced enhancement of AMPAR EPSCs requires raised intracellular [Ca^{2+}], we increased the buffering capacity of the intracellular solution (*17*). With the high Ca^{2+}-buffering solution, EPQ(pY)EEIPIA had no effect on AMPAR EPSCs (Fig. 4A). EPQ(pY)EEIPIA remains active in the high Ca^{2+}-buffering solution because there was an increase in NMDAR EPSCs (Fig. 4, A and B). The increase in NMDAR EPSCs was associated with no change in driving force or in current-voltage (I-V) relationship (Fig. 4B) and was produced with low Ca^{2+}-buffering solution (*18*). Also, the enhancement of NMDA currents by EPQ(pY)-EEIPIA was prevented by Src(40–58) and was not produced by EPQYEEIPIA. Thus, the Src-induced increase in AMPAR EPSCs was Ca^{2+}-dependent, but the potentiation of NMDAR EPSCs was Ca^{2+}-independent.

Because Src is associated with and upregulates the function of NMDA receptors (*7*), we questioned whether NMDA receptors are required for Src-induced enhancement of AMPAR EPSCs. We blocked NMDA receptors by bath-applying the antagonist MK-801 during experiments with low Ca^{2+}-buffering intracellular solution. When MK-801 was applied starting just before whole-cell recording, administration of EPQ(pY)EEIPIA produced no change in EPSP slope (Fig. 4C). In other experiments, after synaptic responses had been potentiated by EPQ(pY)EEIPIA, MK-801 had no effect on AMPAR EPSPs (Fig. 4D). Thus, NMDA receptor activation was necessary to induce, but not to sustain, the Src-induced potentiation of AMPAR-mediated synaptic responses.

Here, blockade of Src prevented induction of LTP and activation of Src, or administration of recombinant Src, induced lasting potentiation that occluded LTP induction. Like tetanus-induced LTP, the potentiation produced by directly activating Src depended on a rise in intracellular [Ca^{2+}] and on NMDARs. Thus, Src fulfills necessary and sufficient conditions to be considered a mediator of LTP induction at Schaffer collateral CA1 synapses. Although there is a basal level of Src function, this did not appear to contribute to LTP, but rather the activation of Src as a consequence of

tetanic stimulation was required to induce LTP (*19*). Thus, activation of Src provides a biochemical mechanism for gating induction of LTP.

Models of biochemical events underlying induction of LTP in hippocampal CA1 neurons focus on the signaling cascades initiated by Ca^{2+} influx through NMDARs (*16*, *20*). The most parsimonious explanation for our findings is that during induction of LTP, Src is rapidly activated, which leads to enhanced NMDAR function. Enhancing NMDAR function results in increased Ca^{2+} entry, which may trigger the downstream signaling cascade. Hence, the present results indicate that for LTP induction there is a hitherto unexpected step upstream of NMDARs (*21*). Src is widely expressed in the nervous system (*22*), and thus Src may have a common role in the plasticity of excitatory synaptic transmission in many regions of the CNS.

REFERENCES AND NOTES

1. T. V. P. Bliss and G. L. Collingridge, *Nature* **361**, 31 (1993); B. Gustafsson and H. Wigstrom, *Trends Neurosci.* **11**, 156 (1988); R. Malenka and R. Nicoll, *ibid.* **16**, 521 (1993).
2. R. Malinow, H. Schulman, R. W. Tsien, *Science* **245**, 862 (1989); R. C. Malenka *et al.*, *Nature* **340**, 554 (1989).
3. T. J. O'Dell, E. R. Kandel, S. G. N. Grant, *Nature* **353**, 558 (1991).
4. S. G. N. Grant *et al.*, *Science* **258**, 1903 (1992).
5. Y. T. Wang and M. W. Salter, *Nature* **369**, 233 (1994); G. Köhr and P. H. Seeburg, *J. Physiol. (London)* **492**, 445 (1996).
6. G. L. Collingridge and W. Singer, *Trends Pharmacol. Sci.* **11**, 290 (1990); R. A. Nicoll and R. C. Malenka, *Nature* **377**, 115 (1995).
7. X.-M. Yu, R. Askalan, G. J. Keil II, M. W. Salter, *Science* **275**, 674 (1997).
8. Methods for preparing slices and for whole-cell and field recording were described in detail previously [Y. M. Lu *et al.*, *J. Neurosci.* **17**, 5196 (1997)]. In brief, hippocampal slices (400 μm) were prepared from 30- to 36-day-old Sprague-Dawley rats and were placed in a holding chamber for at least 1 hour. A single slice was then transferred to a recording chamber where it was continuously superfused with artificial cerebrospinal fluid (ACSF) (2 ml/min) that had been saturated with 95% O_2 and 5% CO_2 at 30° ± 1°C. The composition of ACSF was 124 mM NaCl, 3 mM KCl, 1.25 mM NaH_2PO_4, 1.3 mM $MgCl_2$, 2 mM $CaCl_2$, 26 mM $NaHCO_3$, 10 mM dextrose, and 0.1 mM picrotoxin. For current clamp experiments, the patch pipette (3- to 5-megohm) solution contained 132.5 mM K-gluconate, 17.5 mM $KMeSO_4$, 10 mM Hepes, 0.2 mM EGTA, 2 mM Mg-ATP, 0.3 mM guanosine triphosphate, and 5 mM QX-314 (pH 7.25, 290 mosM). The intracellular solution was supplemented as required with peptides or antibodies that were stored as 100× single-use stock solutions prepared just before use. All peptides used in the study were from J. Bell, Ottawa Regional Cancer Centre, Ottawa, Canada. The peptides and antibodies were numbered and the experimenter (Y.M.L.) was unaware of which was applied in all experiments except those shown in Figs 3 and 4. Patch recordings were done using the "blind" patch method [M. G. Blanton, J. J. LoTurco, A. R. Kriegstein, *J. Neurosci. Methods* **30**, 203 (1989)]. Raw data were amplified with an Axopatch 1-D, sampled at 3 to 6 kHz, and analyzed with Pclamp6 software (Axon Instruments, Foster City, CA). Synaptic responses were evoked by a bipolar tungsten electrode located about 50 μm from the cell bodies. Test stimuli were delivered at a frequency of 0.1 Hz, and the stimulus intensity was set to produce 25% of the maximum response. The tetanic stimulation consisted of two trains of 100-Hz stimulation lasting 500 ms at the intertrain interval of 10 s. In controls, this produced LTP that was at a stable level by 30 min after tetanus and persisted for more than 1.5 hours. For clarity, we show records of only the first 30 min after tetanus. EPSP slope was calculated as the slope of the rising phase 10 to 65% of the peak response. Average EPSP slope values were determined for each 5-min period of recording. The baseline value of EPSP slope was that from the first 5-min period and was defined as 100%. Series resistance ranged from 15 to 19 megohms. Input resistance was monitored every 5 min during the course of all experiments by measurement of responses to 0.2-nA injection for 400 ms. The average value of input resistance was 169 ± 13 megohms. The resting membrane potential was −60 ± 4 mV. Extracellular field potentials were simultaneously recorded with a micropipette filled with ACSF (1 to 3 megohms) placed in the stratum radiatum within 100 μm of the single cell studied. The averaged field EPSP slope was calculated every 1 min.
9. The amino acid sequence of scrambled Src(40–58) was AGSHAPFPSPARAGVAPDA (*13*); it was created by random ordering of the sequence of Src(40–58). With scrambled Src(40–58), EPSP slope increased to 205 ± 13% of baseline [n = 5 cells, $P <$ 0.01 versus Src(40–58)] 30 min after tetanus. As an additional control, Src(40–58) was tested in mice lacking *src* and had no effect on LTP induction (EPSP slope 30 min after tetanus was 195 ± 17% of baseline, n = 5 cells). Src(40–58) prevented LTP in wild-type mice from the same genetic background (EPSP slope was 110 ± 8% of baseline, n = 4 cells), and thus the effect of this peptide required Src.
10. S. Roche, S. Fumagalli, S. A. Courtneidge, *Science* **269**, 1567 (1995). Anti-Src1 was obtained from S. Courtneidge, SUGEN, Redwood City, CA.
11. For voltage-clamp experiments, the patch pipette solution contained 132.5 mM Cs-gluconate, 17.5 mM CsCl, 10 mM Hepes, 0.2 mM EGTA, 2 mM Mg-ATP, 0.3 mM guanosine triphosphate, and 5 mM QX-314 (pH 7.25, 290 mosM). With this solution, the input resistance was 243 ± 19 megohms and series resistance was 20 ± 2 megohms. The holding potential was −60 mV except where otherwise indicated. The amplitude of the AMPAR EPSCs was taken as the peak of the inward current, and the 10 to 90% rise times were 0.6 to 2 ms. This rapid inward current was blocked by bath-applied 6-cyano-7-nitroquinoxaline-2,3-dione (CNQX, 5 μM) and was unaffected by D,L,-2-amino-5-phosphonovaleric acid (APV, 50 μM). NMDAR EPSCs were pharmacologically isolated by bath application of 5 μM CNQX; these EPSCs were abolished by 50 μM APV.
12. Hippocampal slices were prepared and stimulated and extracellular fields were recorded as described above (*8*). After baseline synaptic responses had been stable for at least 10 min, then either tetanic stimulation was delivered or the test stimulation was continued for up to 5 min (control). The CA1 region was microdissected and immediately frozen on dry ice. Four CA1 regions (from a control or from 1 or 5 min posttetanus) were pooled together. In each experiment, an entire set of control, 1-min, or 5-min pooled slices was taken from one animal. For the subsequent preparation and measurement, the experimenter (J.D.) was unaware of the stimulation condition of the pooled slices. The tissue was homogenized in ice-cold lysis buffer containing 50 mM tris-HCl (pH 8.0); 150 mM NaCl; 2 mM EDTA; 1% NP-40; 1 mM Na orthovanadate; protease inhibitors pepstatin A (20 μg/ml), leupeptin (20 μg/ml), and aprotinin (20 μg/ml); and 1 mM phenylmethylsulfonyl fluoride. Insoluble material was removed by centrifugation at 14,000*g* for 10 min at 4°C. The protein content of soluble material was determined by Bio-Rad D_c protein assay. Src activity was measured as Src autophosphorylation by means of an immune complex kinase assay [A. L. Burkhardt and J. B. Bolen, in *Current Protocols in Immunology*, J. E. Coligan, Ed. (Wiley, Boston, 1993), pp. 1–9]. Soluble proteins (100 μg) were pre-cleared with Sepharose beads and then incubated overnight with 2 μl of antibody to Src, monoclonal antibody 327 (J. Bolen, DNAX, Palo Alto, CA). Immune complexes were isolated by addition of 40 μl of protein G–Sepharose beads, followed by incubation for 3 hours at 4°C. Immunoprecipitates were washed five times with lysis buffer. Beads were then resuspended in kinase buffer, which contained 20 mM tris-HCl (pH 7.6), 20 mM $MgCl_2$, 2 mM $MnCl_2$, 1 mM EDTA, 1 mM EGTA, 0.1 mM dithiothreitol, 10 μCi of [γ-^{32}P]ATP, and enolase (3.2 mg/ml). Positive controls containing 0.1, 1, or 10 U of $pp60^{c\text{-}Src}$ (UBI) in kinase buffer were run in parallel. All of the samples were incubated for 5 min at 37°C, and the reaction was stopped by addition of 4× Laemmli sample buffer. Samples were subjected to SDS–polyacrylamide gel electrophoresis (SDS-PAGE; 10% gel). Proteins were transferred to a nitrocellulose membrane and exposed overnight on a Phosphor Screen (Molecular Dynamics, Sunnyvale, CA) for quantitation and analysis with ImageQuant software. Membranes were then immunoblotted with antibody to Src (1:500 dilution); the secondary antibody was coupled to horseradish peroxidase and was visualized by enhanced chemiluminescence.
13. Single-letter abbreviations for the amino acid residues are as follows: A, Ala; C, Cys; D, Asp; E, Glu; F, Phe; G, Gly; H, His; I, Ile; K, Lys; L, Leu; M, Met; N, Asn; P, Pro; Q, Gln; R, Arg; S, Ser; T, Thr; V, Val; W, Trp; and Y, Tyr.
14. X. Liu *et. al.*, *Oncogene* **8**, 1119 (1993). The minimum concentration required to increase Src activity was 1 mM.
15. For perfusion, a pipette (tip diameter, about 10 μm) was inserted into the patch electrode [L. Y. Wang, M. W. Salter, J. F. MacDonald, *Science* **253**, 1132 (1991)]. The perfusion pipette was connected to the microinjection pump, and solutions were injected at a rate of 3 to 5 μl/min.
16. R. Malenka, J. A. Kauer, R. S. Zucker, R. A. Nicoll, *Science* **242**, 81 (1988); R. Malenka, B. Lancaster, R. S. Zucker, *Neuron* **9**, 121 (1992); D. J. Wyllie, T. Manabe, R. A. Nicoll, *ibid.* **12**, 127 (1994).
17. For high Ca^{2+} buffering, the intracellular solution was supplemented with 10 mM EGTA and 1 mM $CaCl_2$.
18. Y. M. Lu, J. C. Roder, J. Davidow, M. W. Salter, data not shown.
19. Experiments showing that LTP is blocked by bath-applied tyrosine kinase inhibitors (*3*) suggest a role for tyrosine kinases in induction of LTP. Mice lacking *src* show LTP in CA1, and LTP is blunted but not abolished in mice lacking the *src* family member *fyn* (*4*). The impairment in LTP is age-dependent in *fyn*$^-$ mice, with *fyn*$^-$ animals 10 weeks or less in age showing LTP comparable to that in wild-type mice [N. Kojima *et al.*, *Proc. Natl. Acad. Sci. U.S.A.* **94**, 4761 (1997)], and the impairment of LTP in the *fyn*$^-$ mice correlates with decreasing levels of Src expression. We suggest that in wild-type individuals, Src is a required mediator for LTP induction, whereas in mutants that develop without *src* it is likely that another member of the *src* family, possibly *fyn*, may substitute for *src* [S. M. Thomas, P. Soriano, A. Imamoto, *Nature* **376**, 267 (1995); P. L. Stein, H. Vogel, P. Soriano, *Genes Dev.* **8**, 1999 (1994)].
20. A. Barria, D. Muller, V. Derkach, L. C. Griffith, T. R. Soderling, *Science* **276**, 2042 (1997); J. Lisman, *Trends Neurosci.* **17**, 406 (1994).
21. The molecular mechanism of enhancement of NMDAR function may be through tyrosine phosphorylation of NMDAR subunit proteins, such as NR2B [I. S. Moon, M. L. Apperson, M. B. Kennedy, *Proc. Natl. Acad. Sci. U.S.A.* **91**, 3954 (1994); J. A. P. Rostas *et al.*, *ibid.* **93**, 10452 (1996); K. Rosenblum, Y. Dudai, G. Richter-Levin, *ibid.*, p. 10457] or NR2A [L. F. Lau and R. L. Huganir, *J. Biol. Chem.* **270**, 20036 (1995)] or associated proteins. It is possible that Src may additionally act by promoting biochemical steps that are downstream of Ca^{2+} entry through NMDARs.
22. J. S. Brugge *et al.*, *Nature* **316**, 554 (1985); R. Martinez, B. Mathey-Prevot, A. Bernards, D. Baltimore, *Science* **237**, 411 (1987).

23. We thank S. Courtneidge and J. Bolen for providing antibodies and J. F. MacDonald, T. Pawson, and Y. T. Wang for critical comments on the manuscript. This work was supported by grants from the Medical Research Council of Canada to J.C.R. and to M.W.S. and by the Nicole Fealdman Memorial Fund (M.W.S.). J.D. was supported by a summer research bursary from Novartis Canada Ltd.

16 October 1997; accepted 6 January 1998